



Petters, S. S., Hilditch, T. G., Tomaz, S., Miles, R. E. H., Reid, J. P., & Turpin, B. J. (2020). Volatility Change During Droplet Evaporation of Pyruvic Acid. *ACS Earth and Space Chemistry*, 4, 741-749. [5].  
<https://doi.org/10.1021/acsearthspacechem.0c00044>

Peer reviewed version

Link to published version (if available):  
[10.1021/acsearthspacechem.0c00044](https://doi.org/10.1021/acsearthspacechem.0c00044)

[Link to publication record in Explore Bristol Research](#)  
PDF-document

This is the author accepted manuscript (AAM). The final published version (version of record) is available online via American Chemical Society at <https://pubs.acs.org/doi/abs/10.1021/acsearthspacechem.0c00044> . Please refer to any applicable terms of use of the publisher.

## University of Bristol - Explore Bristol Research

### General rights

This document is made available in accordance with publisher policies. Please cite only the published version using the reference above. Full terms of use are available:  
<http://www.bristol.ac.uk/red/research-policy/pure/user-guides/ebr-terms/>

This document is confidential and is proprietary to the American Chemical Society and its authors. Do not copy or disclose without written permission. If you have received this item in error, notify the sender and delete all copies.

### Volatility Change During Droplet Evaporation of Pyruvic Acid

Journal:	<i>ACS Earth and Space Chemistry</i>
Manuscript ID	Draft
Manuscript Type:	Article
Date Submitted by the Author:	n/a
Complete List of Authors:	Petters, Sarah; University of North Carolina at Chapel Hill, Environmental Sciences and Engineering Hilditch, Thomas; University of Bristol, School of Chemistry Tomaz, Sophie; IRCELYON Miles, Rachael; University of Bristol, School of Chemistry Reid, Jonathan; University of Bristol, School of Chemistry Turpin, Barbara; University of North Carolina at Chapel Hill Gillings School of Global Public Health, Department of Environmental Science and Engineering;

SCHOLARONE™  
Manuscripts

Manuscript for submission to *ACS Earth and Space Chemistry*

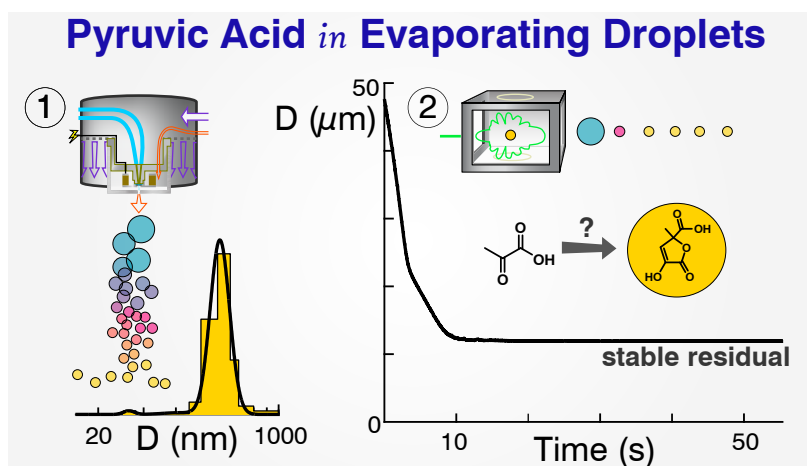
# Volatility Change During Droplet Evaporation of Pyruvic Acid

Sarah S. Petters,<sup>1\*</sup> Thomas G. Hilditch,<sup>2</sup> Sophie Tomaz,<sup>1,†</sup> Rachael E. H. Miles,<sup>2</sup> Jonathan P. Reid,<sup>2</sup>  
and Barbara J. Turpin<sup>1</sup>

<sup>1</sup>Department of Environmental Sciences and Engineering, Gillings School of Global Public  
Health, University of North Carolina at Chapel Hill, Chapel Hill, North Carolina, USA

<sup>2</sup>School of Chemistry, University of Bristol, Bristol BS8 1TS, UK

Manuscript for submission to ACS Earth and Space Chemistry. Feb. 11, 2020.



TOC art

Manuscript for submission to *ACS Earth and Space Chemistry*

## 12 **Abstract**

13 Atmospheric water-soluble organic gases such as pyruvic acid are produced in large quantities by  
14 photochemical oxidation of biogenic and anthropogenic emissions and undergo water-mediated  
15 reactions in aerosols and hydrometeors. These reactions can contribute to aerosol mass by forming  
16 less volatile compounds. While progress is being made in understanding the relevant aqueous  
17 chemistry, little is known about the chemistry that takes place during droplet evaporation. Here we  
18 examine the evaporation of aqueous pyruvic acid droplets using both the Vibrating Orifice Aerosol  
19 Generator (VOAG) and an electrodynamic balance (EDB). In some cases pyruvic acid was first  
20 oxidized by OH radicals. The evaporation behavior of oxidized mixtures was consistent with  
21 expectations based on known volatilities of reaction products. However, independent VOAG and  
22 EDB evaporation experiments conducted without oxidation also resulted in stable residual  
23 particles; the estimated volume yield was 10–30% of the initial pyruvic acid. Yields varied with  
24 temperature and pyruvic acid concentration across cloud, fog, and aerosol-relevant concentrations.  
25 The formation of low volatility products, likely cyclic dimers, suggests that pyruvic acid accretion  
26 reactions occurring during droplet evaporation could contribute to the gas-to-particle conversion  
27 of carbonyls in the atmosphere.

## 28 **1. Introduction**

29 Aerosols affect global climate and impact air quality, human health, and visibility. A substantial  
30 fraction of aerosol mass is organic, much of which is formed in-situ in the atmosphere. Despite its  
31 ubiquity, predictions of secondary organic aerosol (SOA) formation rely on incomplete  
32 mechanisms unlikely to capture aerosol production over a wide range of precursors and  
33 conditions.<sup>1–3</sup> Water-mediated reactions, occurring in humidified aerosols, fogs, and cloud  
34 droplets, play an important role in converting water-soluble organic gases (WSOGs) to SOA

Manuscript for submission to *ACS Earth and Space Chemistry*

35 mass.<sup>4-6</sup> However, the contribution of aqueous reactions to SOA mass remains uncertain due in  
36 part to a limited understanding of precursors and limited laboratory results to parameterize  
37 models.<sup>1,7-11</sup> Quantifying the impacts of aqueous and multiphase chemistry on aerosol mass  
38 remains challenging, and a more detailed understanding of product volatility is needed.

39 A significant fraction of low molecular weight acids, aldehydes and carbonyls dissolve into  
40 cloud or fog droplets. In the absence of additional reactions, these WSOGs largely evaporate  
41 during water evaporation; the trace amounts that remain in the aerosol phase are determined by  
42 their partial pressure in the gas phase and activity in the aerosol matrix. However, multiphase  
43 reactions can generate low-volatility products that are retained in the equilibrated aerosol. Several  
44 important criteria determine whether aqueous processing can appreciably increase SOA mass: (1)  
45 the precursor must be abundant, (2) it must have a high vapor pressure before aqueous reactions,  
46 (3) it must have a high Henry's law coefficient and thus strongly partition into water, and (4) it  
47 must react in the aqueous phase to form less volatile products.

48 To date many cloud- and fog-relevant studies have focused on the aqueous OH oxidation of a  
49 limited number of compounds meeting the above criteria, such as glyoxal,<sup>12-14</sup> glycolaldehyde,<sup>15,16</sup>  
50 methacrolein,<sup>17</sup> acetic acid,<sup>18</sup> methylglyoxal,<sup>19-21</sup> methyl vinyl ketone,<sup>22</sup> phenolic compounds,<sup>23</sup>  
51 and pyruvic acid,<sup>24,25</sup> as well as studies focusing on oxidation by singlet molecular oxygen<sup>23</sup> and  
52 triplet excited states of oxygen,<sup>23,26</sup> photosensitization,<sup>27</sup> and photoinitiation.<sup>28</sup> The volatility of the  
53 products, or the extent to which products remain in the particle phase after water evaporation, has  
54 been determined for some of these systems but not for pyruvic acid. Studies have also shown that  
55 non-radical reactions can yield low-volatility compounds in deliquescent aerosols,<sup>29-32</sup> especially  
56 for glyoxal, methylglyoxal, and isoprene-derived epoxydiols.<sup>29-32</sup> Because these systems rely on  
57 catalysis, formation of oligomers is sometimes reversible; irreversible formation of low-volatility

Manuscript for submission to *ACS Earth and Space Chemistry*

1  
2  
3 58 products are generally associated with radical<sup>4,33,34</sup> or ring-opening<sup>31</sup> reactions due to their higher  
4  
5 59 activation energy. Nevertheless, glyoxal and methylglyoxal form stable products in evaporating  
6  
7 60 solutions with or without inorganic catalysts<sup>30,32,35</sup> due to the reactive dicarbonyl group.<sup>35</sup> These  
8  
9 61 and other accretion reactions occurring in the absence of photooxidation have been recognized as  
10  
11 62 an important contributor to organic aerosol.<sup>36</sup> Evaporation of droplets concentrates solutes, shifts  
12  
13 63 the solution pH, and can allow enhanced surface partitioning of surface-active compounds over  
14  
15 64 short timescales, enhancing reaction rates.<sup>32,37-41</sup> The droplet air-liquid interface may also  
16  
17 65 accelerate reactions by confining molecules to specific orientations, enhancing their reactivity or  
18  
19 66 acidity,<sup>42-46</sup> and molecular partitioning to the air-liquid interface and self-organization in the  
20  
21 67 surface layer can affect gas uptake and reaction rates.<sup>47,48</sup>  
22  
23  
24  
25  
26

27 68 Pyruvic acid is abundant in aerosols, fogs, and clouds, and is produced<sup>19,24,25,49,50</sup>  
28  
29 69 photochemically in the atmosphere<sup>50,51</sup> mainly through gas-phase oxidation of aromatic  
30  
31 70 hydrocarbons,<sup>52-54</sup> biomass burning,<sup>55</sup> and aqueous OH oxidation of methylglyoxal.<sup>49,56</sup> Pyruvic  
32  
33 71 acid has an intermediate volatility<sup>34</sup> and partitions between the gas and aerosol phases.<sup>51,53,57</sup>  
34  
35 72 Studies of aqueous pyruvic acid processing have focused on photolysis<sup>26,56,58</sup> and OH-radical  
36  
37 73 initiated photooxidation.<sup>24,25,59</sup> Evidence for dark pyruvic acid accretion reactions from  
38  
39 74 environmental chamber studies shows that partitioning of pyruvic acid and other acids or carbonyls  
40  
41 75 to SOA exceeds expectations based on their high vapor pressures.<sup>52,60</sup> Here we extend these studies  
42  
43 76 to include dark processing of pyruvic acid in evaporating cloud droplets.  
44  
45  
46  
47  
48

49 77 In this work we examine an aspect of cloud/fog processing – the evolving volatility distribution  
50  
51 78 of aqueous pyruvic acid with droplet evaporation. We also investigate changes in volatility after  
52  
53 79 OH oxidation of the aqueous pyruvic acid solutions.  
54  
55  
56  
57

## 80 **2. Method**

81 Pyruvic acid evaporation experiments followed two methods and spanned concentration ranges  
82 from 10  $\mu\text{M}$  to 2 M. Vibrating Orifice Aerosol Generator (VOAG)<sup>61</sup> Evaporation and Residual  
83 Analysis (VERA) was performed for a series of solutions between 10  $\mu\text{M}$  (cloud relevant) and 20  
84 mM, a concentration range that reflects cloud concentrations and concentrations as cloud droplets  
85 evaporate. Additional pyruvic acid evaporation experiments were performed using an  
86 electrodynamic balance (EDB) at 2 M. The EDB concentration is relevant to deliquescent aerosols  
87 rather than clouds; the choice of concentrations for EDB experiments was dictated by instrumental  
88 constraints. For comparison, VERA experiments were also performed for other organic acids (10  
89  $\mu\text{M}$ –20 mM) and for aqueous pyruvic acid after OH-radical oxidation (300  $\mu\text{M}$  pyruvic acid; fog-  
90 relevant concentration). An evaporation model was used to aid in the interpretation of data. VERA  
91 and EDB techniques, oxidation experiments, and modeling are described in the following  
92 paragraphs.

### 93 **2.1 VOAG Evaporation and Residual Analysis (VERA)**

94 Droplet evaporation experiments were performed for aqueous solutions of pyruvic acid (with  
95 and without OH oxidation) or other organic acids/carbonyls using VERA as described  
96 previously.<sup>16</sup> VERA emulates cloud droplet evaporation by generating micron-scale droplets with  
97 very narrow size distributions (monodispersed and near cloud-relevant sizes),<sup>62</sup> and evaporating  
98 them in a turbulent flow tube. Briefly, a VOAG (TSI 3450) was used to generate monodisperse  
99 droplets. Water evaporated rapidly and size distributions of the organic residuals were detected in  
100 real time downstream by an aerosol spectrometer (GRIMM Aerosol Technik Ainring GmbH;  
101 model 1.109). Evaporation of the organic served as a metric of its vapor pressure. Modifications  
102 to the instrument liquid feed, orifice, and flow tube following Barr et al.<sup>63–65</sup> are described in the

Manuscript for submission to *ACS Earth and Space Chemistry*

1  
2  
3 103 Supporting Information (SI) alongside the measurement schematic (Figure S1); analysis is  
4  
5 104 described below. A 20  $\mu\text{m}$  orifice was used and produced  $35\pm 0.053$   $\mu\text{m}$  droplets under typical  
6  
7 105 conditions. For an involatile solute, solutions of 9.4  $\mu\text{M}$  to 19 mM result in dry residual diameters  
8  
9 106 (hereafter referred to as “nominal diameters”) of 0.30 to 3.9  $\mu\text{m}$ . Equilibrium water retention was  
10  
11 107 estimated from molar volume<sup>66,67</sup> and did not exceed 2–5% of nominal particle volume.  
12  
13 108 Calculation details and spectrometer calibration are described in the SI. Observed residual  
14  
15 109 diameters were taken as the peak of the measured size distribution. The evaporation process and  
16  
17 110 the influence of physicochemical properties are described in the Evaporation Modeling section  
18  
19 111 below.

## 25 112 **2.2 Evaporation in the Electrodynamic Balance (EDB)**

26 113 Pyruvic acid solutions were evaporated in an EDB as described previously.<sup>68–70</sup> Aqueous  
27  
28 114 solutions of 2 M pyruvic acid in ultrapure water were prepared. The higher concentration was  
29  
30 115 necessary due to experimental constraints and is comparable to total organic carbon (TOC) in  
31  
32 116 deliquescent aerosols.<sup>71</sup> Droplets were produced using a piezoelectric droplet-on-demand  
33  
34 117 generator and trapped in an electrodynamic potential well generated from two pairs of concentric  
35  
36 118 cylindrical electrodes. Trapped droplets evaporated in a 3  $\text{cm s}^{-1}$   $\text{N}_2$  gas flow at constant  
37  
38 119 temperature and relative humidity (RH). A green laser (532 nm) illuminated the droplet and the  
39  
40 120 scattered diffraction pattern was used to determine droplet size with a time resolution of 10 ms.  
41  
42 121 Experiments were performed at 10, 20, and 25°C. Additional tests included variable RH or a  
43  
44 122 different initial solvent. EDB experiments were conducted at the University of Bristol. Each  
45  
46 123 experiment was repeated 4–9 times.



Manuscript for submission to *ACS Earth and Space Chemistry*

### 124 **2.3 Oxidation and Product Quantification for Pyruvic Acid + OH(aq)**

125 Aqueous solutions of 300  $\mu\text{M}$  (10.8 ppm-C) pyruvic acid were oxidized via OH radicals using  
126 a water-jacketed 1 L photochemical batch reactor at 25°C as described previously and products  
127 were quantified by ion chromatography.<sup>19,72</sup> The pyruvic acid concentration is similar to the total  
128 organic carbon found in fog water or polluted cloud water.<sup>73,74</sup> Estimated steady-state [OH] was  
129  $\sim 5.5 \times 10^{-12}$  M during pyruvic acid oxidation.<sup>75</sup> Additional experimental details are provided in the  
130 SI. Typical cloudwater [OH] is believed to be  $10^{-13}$  M or lower.<sup>76,77</sup> We used higher concentrations  
131 to focus on OH initiated reactions and to access a wide range of equivalent atmospheric oxidation  
132 timescales from minutes to days.<sup>76</sup>

133 Aliquots of 10–12 mL were withdrawn at increasing time intervals and offline analysis was  
134 performed within one day. Samples were analyzed for organic acids using ion chromatography  
135 (IC; Dionex ICS-3000) and for TOC (Sievers M9). Evaporation experiments using VERA were  
136 performed for a subset of aliquots directly and after serial dilution.

## 137 **3. Evaporation Model**

138 Evaporation of pyruvic acid solution droplets in VERA was estimated following Su et al.<sup>70,78</sup>  
139 and Bilde et al.<sup>79,80</sup> A model description is included in the SI. Particle velocity relative to the gas  
140 was assumed to be the terminal settling velocity<sup>80</sup> and the gas-phase concentration of organic was  
141 assumed to be zero in the flow tube (we estimate it was < 2% saturated). Pyruvic acid diffusivity  
142 in air was estimated to be  $8.1 \times 10^{-2}$   $\text{cm}^2 \text{ s}^{-1}$  via the Hirschfelder equation.<sup>79,81,82</sup> VERA was  
143 emulated by modeling water evaporation from the droplet until reaching the organic nominal  
144 residual diameter, then modeling organic evaporation until the time of observation by the  
145 spectrometer. Modeled RH was 11% and measured RH was 10–13%. In addition to modeling  
146 binary water-organic solutions, we modeled scenarios introducing a second solute with lower

Manuscript for submission to *ACS Earth and Space Chemistry*

1  
2  
3 147 vapor pressure ( $10^{-4}$  Pa) into the droplet. The modeled residual diameter is mainly controlled by  
4  
5 148 aqueous solution concentration, organic vapor pressure, evaporation time and RH.

6  
7  
8 149 Figure S2 shows the evaporation model for the VERA technique. After water evaporation the  
9  
10 150 “nominal diameter” of the residual organic particle is calculated from the initial solution  
11  
12 151 concentration assuming no evaporation of the organic (x-axis). However, because the organic  
13  
14 152 matter partially evaporates, the “observed diameter” (residual diameter observed by the  
15  
16 153 spectrometer), on the y-axis, is dependent on the organic vapor pressure. Panel A shows the  
17  
18 154 expected observation for a pyruvic acid-like compound with different assigned vapor pressures.  
19  
20 155 The line spacing shows the vapor pressure resolution for organics of similar size and functionality.  
21  
22 156 Vapor pressures ( $p^o$ ) between 3 and 0.3 Pa are resolved under current operating conditions. Panel  
23  
24 157 B shows the result of adding an involatile second solute to the modeled droplets, simulating the  
25  
26 158 conversion of some of the pyruvic acid to a less volatile compound. The inset is a three-bin  
27  
28 159 volatility basis set for this setup, where bin 1 ( $p^o \leq 0.3$  Pa) describes compounds that do not  
29  
30 160 evaporate, bin 2 ( $0.3 \leq p^o \leq 3$  Pa) describes compounds that partially evaporate, and bin 3 ( $p^o \geq 3$   
31  
32 161 Pa) describes compounds evaporating completely before detection.  
33  
34  
35  
36  
37  
38

39 162 Figure S2 shows the droplet size after 4.9 s of evaporation (the flow tube residence time), to  
40  
41 163 simulate what is measured by VERA. It does not show the time-resolved evaporation of multiple  
42  
43 164 solution components because VERA uses a fixed observation time and multiple experiments with  
44  
45 165 different concentrations to generate a plot of nominal vs observed diameter. The model is therefore  
46  
47 166 helpful in interpreting the data. The presence or absence of curvature in the observations is an  
48  
49 167 indication of the volume fraction of solute in each of the volatility bins shown in Panel B. If  
50  
51 168 observations include curvature, some component falls in bin 2 and its vapor pressure can be  
52  
53 169 determined with greater precision. In the absence of curvature, all components are in bins 1 and 3,  
54  
55  
56  
57  
58  
59  
60

Manuscript for submission to *ACS Earth and Space Chemistry*

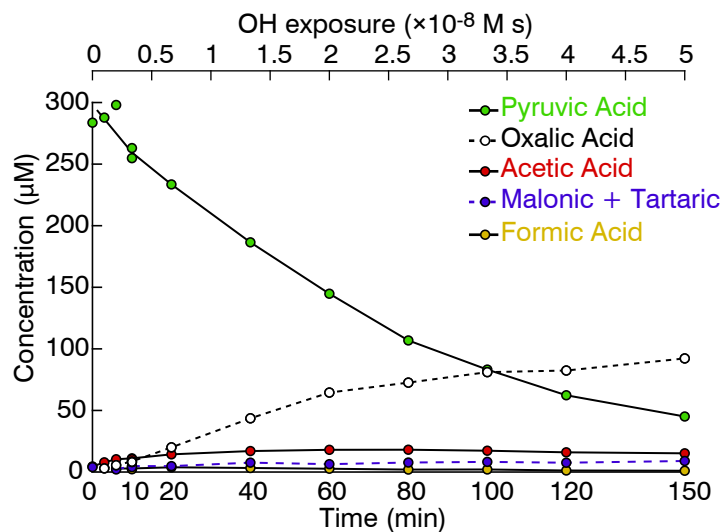
1  
2  
3 170 with the fraction in bin 1 shown by the angle of the line of observed diameters. For example, if the  
4  
5 171 angle is  $0^\circ$  (x-axis), all compounds are in bin 3 (evaporated), and if the angle is  $45^\circ$  (1:1 line), all  
6  
7  
8 172 compounds are in bin 1 (did not evaporate). Evaporation data (nominal vs observed residual  
9  
10 173 diameter) falling on a line between  $0^\circ$  and  $45^\circ$  in Figure S2 panel B are fitted and the slope of the  
11  
12 174 fit line is indicative of the fraction of organic that did not evaporate.

## 16 175 **4. Results and Discussion**

17  
18 176 In the following paragraph we show that OH oxidation of pyruvic acid slowly produces acetic  
19  
20 177 and oxalic acids, consistent with known mechanisms, and that oxidation reduces the volatility of  
21  
22 178 the mixture. Then we present the dark evaporation of aqueous pyruvic acid using VERA and EDB  
23  
24 179 techniques. Despite expectations based on the vapor pressure of pyruvic acid, droplet evaporation  
25  
26  
27 180 resulted in the formation of stable residual particles. A possible oligomerization mechanism and  
28  
29 181 atmospheric implications are discussed.

### 32 182 **4.1 Oxidation Experiments**

33  
34 183 Figure 1 shows the evolving composition of 300  $\mu\text{M}$  aqueous pyruvic acid undergoing OH  
35  
36 184 radical-initiated oxidation over 150 min, as determined by ion chromatography. Oxidation  
37  
38 185 converts pyruvic acid mainly to oxalic and acetic acid. This delayed formation of oxalic acid is  
39  
40 186 consistent with the known multistep oxidation mechanisms.<sup>19,75,83</sup> Evaporation of these solutions  
41  
42  
43 187 and their volatility is discussed below.

Manuscript for submission to *ACS Earth and Space Chemistry*

188

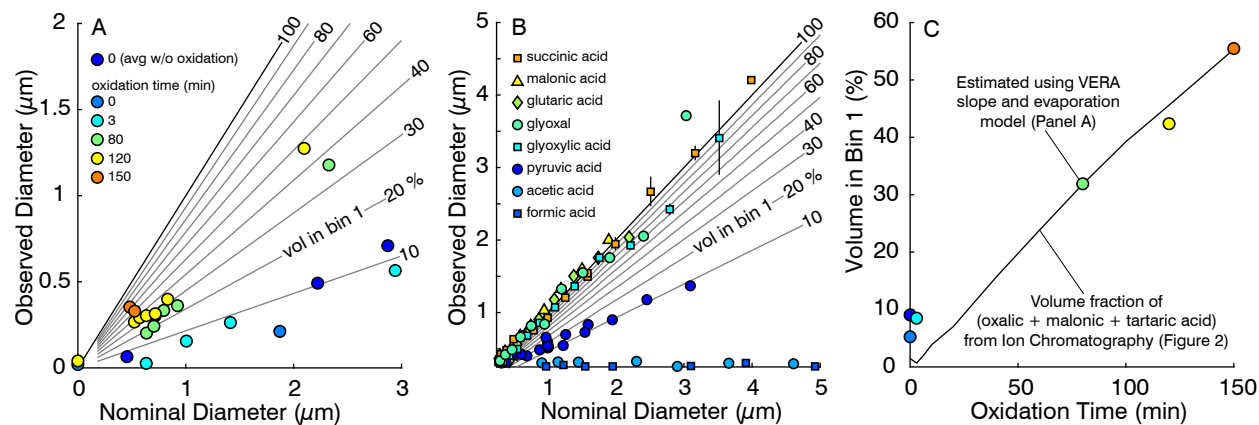
189 **Figure 1.** Oxidation products of pyruvic acid + OH(aq) as quantified by ion chromatography.

#### 190 4.2 VERA Evaporation Experiments

191 Figure 2 shows the results of VERA experiments for oxidized pyruvic acid and for (dark)  
 192 standard solutions of pyruvic acid or other organics. As oxidation converts pyruvic acid to oxalic  
 193 acid, the net result is lower volatility, as seen by an increase in the slope of Figure 2A. By  
 194 comparing the slope of the observations with the modeled lines we estimate that the volume  
 195 fraction of organics in volatility bin 1 ( $p^o < 0.3$ ) was  $\sim 60\%$  after 150 min of oxidation. The  
 196 remaining 40% was likely unreacted pyruvic acid and volatile products such as acetic and formic  
 197 acids. Panel B shows evaporated standard solutions. Most organics longer than 3 carbons did not  
 198 evaporate before observation and thus fall in bin 1 and are observed on the 1:1 line. Additional  
 199 experiments falling on the 1:1 line were omitted for clarity (oxalic, tartaric, and malic acids).  
 200 Compounds evaporating completely fall in bin 3 ( $p^o > 3$ ) and are observed on the x-axis. Pyruvic  
 201 acid solutions evaporated partially (dark blue). As described in section 3, the lack of curvature in  
 202 the observation indicates that some of the solute was volatile (pyruvic acid falls in volatility bin 3)  
 203 and some of the solute did not evaporate (unknown compound falling in volatility bin 1). Assuming

Manuscript for submission to *ACS Earth and Space Chemistry*

204 volume additivity,  $\sim 10 \pm 5\%$  of the pyruvic acid by volume was converted to a lower volatility  
 205 product. The volume conversion is likely lower when accounting for solvation effects.

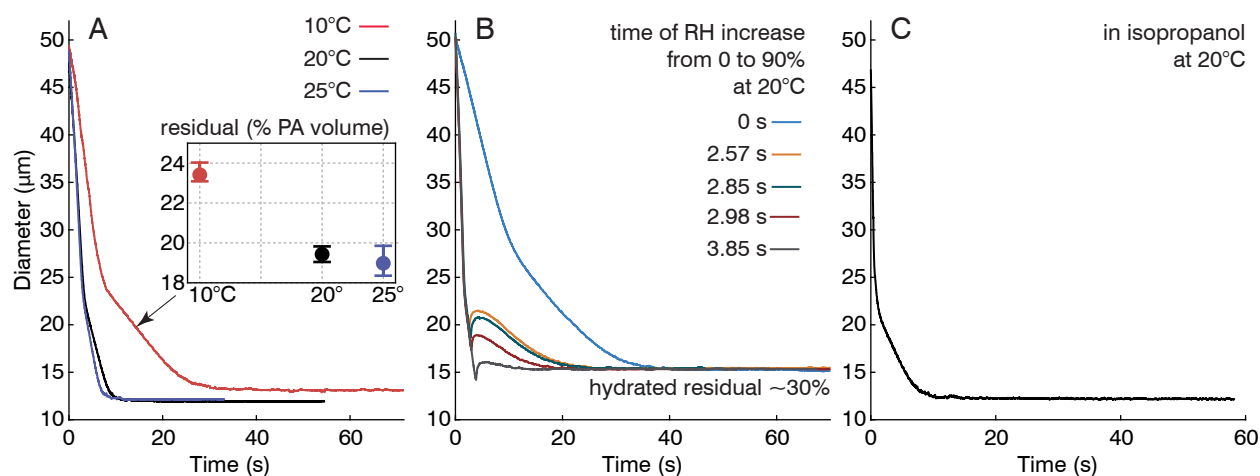


206 **Figure 2.** VERA evaporation of (A) oxidized pyruvic acid solutions (background subtracted) and  
 207 (B) aqueous pyruvic acid and other compounds. Observed diameter is by spectrometer and  
 208 nominal diameters are involatile-equivalent diameters from solution concentration. Grey lines  
 209 show estimated fraction with lower volatility (volatility bin 1;  $p^o < 0.3$  Pa). (C) Percentage of  
 210 solute in bin 1 ( $p^o < 0.3$ ) estimated independently from VERA slope (circles; data from panel A)  
 211 and from IC data (line; data from Figure 1).

213 Figure 2C shows that oxidation shifted products into the lower-volatility bin (bin 1). Colored  
 214 circles indicate the fitted slope of VERA experiments in Panel A and the black line is an  
 215 independent estimate of non-evaporating compounds for the same mixtures using ion  
 216 chromatography, shown in Figure 1. The close agreement between these two estimates of  
 217 evaporation corroborates the VERA model. The exception is near 0 minutes of oxidation, where  
 218 evaporation of the pyruvic acid produced a 10% unknown residual (see blue circles, Figure 2C).  
 219 Further experiments investigating this phenomenon were performed using the EDB and are  
 220 detailed below.

### 221 4.3 EDB Evaporation Experiments

222 Figure 3 shows the evaporation of pyruvic acid solutions in the EDB. The sequential  
 223 evaporation of water, pyruvic acid, and an unknown low-volatility substance is clearly delineated  
 224 by two sharp changes in evaporation rate (Panel A). Evaporation rate slowed as remaining droplet  
 225 constituents became less volatile. Abruptly raising the RH did not change the final residual  
 226 diameter (Panel B). In the evaporation of pyruvic acid + isopropanol (Panel C) the sequential  
 227 evaporation of solvent and pyruvic acid is also observed, again resulting in a less volatile residual.  
 228 The volume conversion of pyruvic acid to low-volatility residual (assuming volume additivity and  
 229 constant density equal to that of pyruvic acid) was ~15–30% across all EDB experiments.



230  
 231 **Figure 3.** Evaporation of 0.1 mass fraction pyruvic acid solution droplets as observed by the EDB.  
 232 (A) aqueous pyruvic acid evaporating in dry  $\text{N}_2$  at three gas-phase temperatures. (inset) residual  
 233 volumes at different temperatures. (B) aqueous pyruvic acid response to abruptly increasing RH  
 234 during evaporation (at different times as indicated), (C) pyruvic acid in isopropanol evaporating at  
 235 20°C.

236 Varying experimental conditions affected the production of the low-volatility component.  
 237 Figure 3A shows that the residual mass of low-volatility product increases at colder temperatures,  
 238 demonstrating that the sustained period of high pyruvic acid concentration in the evaporating  
 239 droplet has a greater effect on the reaction rate than the reduction in molecular collisions expected

Manuscript for submission to *ACS Earth and Space Chemistry*

240 at low temperatures. The volatility of the residual remained below the limit of quantification by  
241 EDB ( $<5 \times 10^{-3}$  Pa) at all temperatures. Additional experiments operating on much longer  
242 timescales would have been necessary to quantify the evaporation of the formed particles.  
243 Although vapor pressure increases with increasing temperature, the effect of temperature-  
244 dependent vapor pressure on the evaporation of a single compound would result in different  
245 evaporation rates and not different yields. Comparison at different initial droplet concentrations  
246 (VERA vs EDB) shows a modest enhancement in volumetric yield at higher initial concentration.  
247 When RH was increased from 0% to 90% at different times during droplet evaporation (Figure  
248 3B), the observed residual diameter was unchanged. Note that the residual here is larger due to  
249 equilibrium water uptake (hygroscopicity estimate of  $\kappa \sim 0.015$ ,<sup>84</sup> which comparable to that of  
250 larger molecules found in SOA<sup>85</sup>). This indicates that changing the hygroscopically-bound water  
251 in the evaporating pyruvic acid solution does not speed up the low-volatility product formation. In  
252 Panel C, evaporating the pyruvic acid in pure isopropanol resulted in evaporation rates and  
253 residuals similar to those of aqueous solutions. Because carbonyls do not undergo hydration  
254 reactions to form gem-diols as readily in isopropanol as they do in water, this suggests that the  
255 reaction producing the residual is not accelerated by the formation of a gem-diol as observed for  
256 glyoxal.<sup>35</sup>

#### 257 **4.4 Proposed Mechanism for Self-Reaction of Pyruvic Acid**

258 Potential formation mechanisms and structures of a low-volatility residual are now discussed.  
259 The residual volume is larger than the stated pyruvic acid impurity of 2% (all EDB experiments  
260 used brand-new stock), and several independent sources of pyruvic acid standards produced  
261 similar results. Some of this residual may form in the stock solution prior to use; however, the  
262 changing volumetric yields with changing temperatures suggests that reactions occur during

Manuscript for submission to *ACS Earth and Space Chemistry*

263 evaporation experiments. Evaporation rates of the low volatility residual were below detection,  
264 thus the influence of temperature on vapor pressure did not affect the observed yield. Gas-phase  
265 impurities are ruled out with the EDB and are unlikely with VERA.

266 Pyruvic acid exists as several species in solution and these equilibria are shifted by the changing  
267 pH during evaporation. The carboxylic acid group can deprotonate to form the pyruvate anion and  
268 the keto group can hydrate to form a gem-diol or tautomerize to form an enol. At room temperature,  
269 roughly 10% of pyruvate, or 60% of pyruvic acid, forms a diol.<sup>86</sup> Equilibrium between these forms  
270 of pyruvic acid is complicated by the high surface-to-volume ratio and rapid removal of both water  
271 and the volatile carboxylic acid form of pyruvic acid during evaporation of droplets.<sup>37,42,44</sup>

272 The formation of C–O–C bonds by attack of an ROH group on the double bond of either the  
273 carboxyl group or the keto group of pyruvic acid is plausible. For example, acid-catalyzed  
274 esterification may convert the carboxyl group to an ester. In this reaction, the gem-diol of a  
275 hydrated pyruvic acid molecule attacks the double bond of the carboxyl group of another pyruvic  
276 acid molecule. In isopropanol, the isopropanol can attack the carboxyl double bond, producing a  
277 similar ester (Figure 3C). Either isopropanol or the pyruvic gem-diol may attack the hydrated keto  
278 group of another pyruvic acid molecule, forming a hemiacetal and potentially repeating to form an  
279 acetal, as has been reported for glyoxal.<sup>87</sup> An acetal may be stable against hydrolysis upon the  
280 removal of pyruvic acid and water from the droplet.

281 Aldol addition and condensation reactions occur by the attack of the enol tautomer of pyruvic  
282 acid on a protonated keto group of another molecule. Figure S3 shows a proposed mechanism with  
283 a cyclic dimer as a potential end product of the aqueous evaporation experiments in this work.  
284 Pyruvic acid tautomerizes readily in solution,<sup>88</sup> and aldol addition can proceed without hydration  
285 of the keto group to a gem-diol. Self-reactions by aldol addition have been reported for



Manuscript for submission to *ACS Earth and Space Chemistry*

286 methylglyoxal and glyoxal<sup>30</sup> and for pyruvic acid in both dark and photochemical reaction  
287 systems.<sup>56,89</sup>

#### 288 **4.5 Atmospheric Implications**

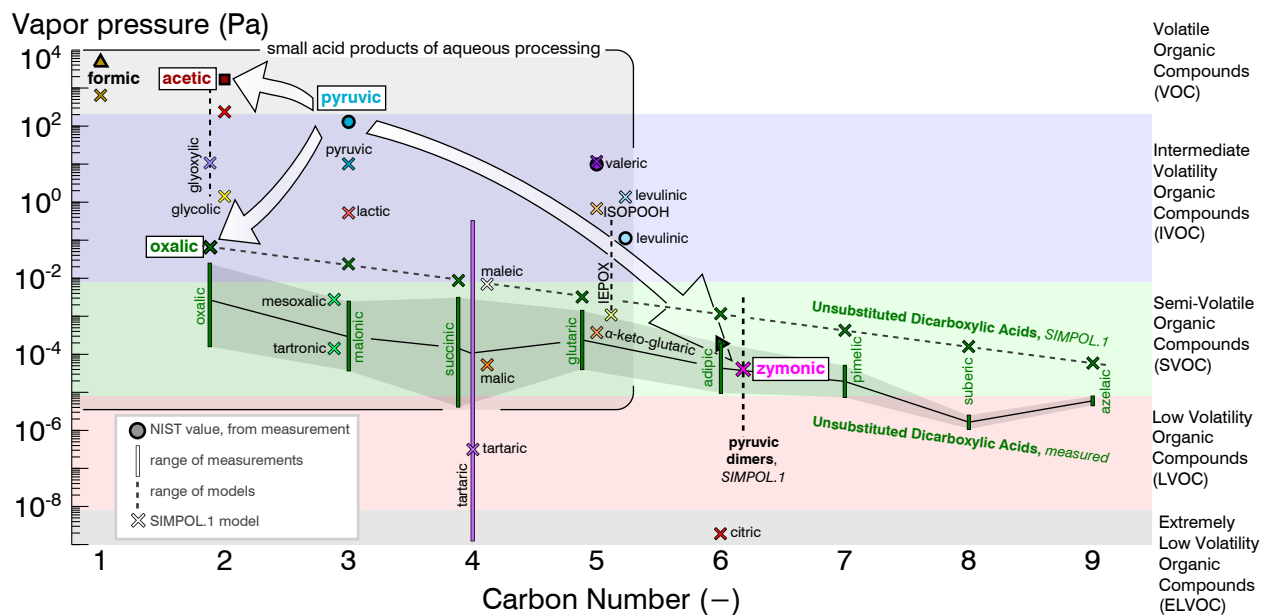
289 Pyruvic acid has diverse removal processes in the atmosphere, where it can partition between  
290 aerosol, aqueous, and gas phases and can dissociate, hydrate, or tautomerize in solution. The  
291 primary source of pyruvic acid outside of urban areas is the aqueous phase OH oxidation of  
292 isoprene oxidation products such as methylglyoxal and lactic acid,<sup>19,57,90</sup> and under dry conditions  
293 it is found largely in gas phase (rather than the aerosol), where it is removed by direct photolysis  
294 and dry deposition.<sup>51,53,91</sup> In the presence of fogs and clouds pyruvic acid can be retained by (or  
295 re-partition back into) the aqueous phase due to its high water solubility (Henry's law constant of  
296  $3.1 \times 10^5 \text{ M atm}^{-1}$ ).<sup>92</sup> The aqueous phase photochemistry is then competitive with the gas-phase  
297 direct photolysis as a sink for pyruvic acid.<sup>93</sup> In clouds and fogs, some pyruvic acid undergoes OH  
298 oxidation to yield acetic acid, CO<sub>2</sub>, and oxalic acid through a glyoxylic acid intermediate.<sup>19</sup>  
299 Because of the multistep chemistry, conversion of pyruvic to oxalic acid takes hours and occurs  
300 over multiple cloud cycles or in a persistent fog. Aqueous dehydrated pyruvic acid is light-  
301 absorbing and can undergo direct photolysis or photosensitized reactions resulting in acetoin, lactic  
302 and acetic acid, and oligomers through the excited triplet state of the carbonyl oxygen.<sup>26,28</sup>  
303 However, dark reactions in clouds and fogs can also occur. Dicarboxyls similar to pyruvic acid  
304 such as glyoxal and methylglyoxal can oligomerize in evaporating droplets.<sup>29,30,32,35,94</sup> This work  
305 shows the potential for pyruvic acid to oligomerize during cloud and fog droplet evaporation.

306 Figure 4 depicts the volatility evolution of aqueous solutions of pyruvic acid. The box in the  
307 upper left-hand corner shows volatile and semivolatile carboxylic acids that are highly water  
308 soluble, often result from aqueous oxidation, and partition readily into droplets. Processes reducing

Manuscript for submission to *ACS Earth and Space Chemistry*

309 the volatility of these compounds can increase the fraction of organic mass that remains in the  
310 particle phase after water evaporation. Among these is pyruvic acid, with a vapor pressure of  $\sim 10^2$   
311 Pa at 20°C.<sup>95,96</sup> Aqueous OH-radical initiated oxidation, dark acid-catalyzed accretion reactions  
312 and, salt formation of pyruvic acid (not shown) have the potential to reduce the volatility of pyruvic  
313 acid. Aqueous OH oxidation of pyruvic acid forms acetic acid, glyoxylic acid, and subsequently  
314 oxalic acid, whose vapor pressure is in the semivolatile range ( $p^o = 10^{-2}$  to  $10^{-4}$  Pa).<sup>97,98</sup> The  
315 preference of oxalic acid for the particle phase in the atmosphere is likely due to the formation of  
316 low volatility oxalate salts or complexes.<sup>4,12,99</sup> This work suggests that evaporating pyruvic acid  
317 solution droplets at aerosol, fog, cloud-relevant concentrations and atmospheric temperatures (10–  
318 25°C), in the absence of an inorganic catalyst, leads to formation of acetals and/or cyclic dimers  
319 with estimated vapor pressures of  $4 \times 10^{-5}$  Pa<sup>100</sup> and 10–30% volumetric yields. This mechanism  
320 could compete with photochemical sinks for pyruvic acid during cloud cycling under dark  
321 conditions.

322 Although the vapor pressure of dimers of pyruvic acid is significantly lower than that of pyruvic  
323 acid, they are still considered semivolatile. Dimerization enhances the partitioning of monomers  
324 to the condensed phase.<sup>36</sup> The formed dimers, especially those with unsaturated double bonds, can  
325 participate in additional condensed-phase reactions. For example, the pyruvic acid dimers shown  
326 in Figure S5 have been shown to partition to the air-water interface,<sup>101</sup> where they may have  
327 enhanced reactivity for subsequent reactions.<sup>38</sup> The formation of surface active unsaturated dimers  
328 from carbonyls such as pyruvic acid during cloud or fog evaporation is one way in which carbon  
329 can be transformed in the atmosphere and influence atmospheric chemistry.

Manuscript for submission to *ACS Earth and Space Chemistry*

330

331 **Figure 4.** Vapor pressures of pyruvic acid reaction products compared to past organic  
 332 measurements (20°C),<sup>102</sup> SIMPOL.1<sup>100</sup>-estimated vapor pressures, and volatility ranges defined  
 333 by Donahue et al.<sup>34</sup> Pyruvic dimers include several multifunctional cyclic acids (Figure S3).

Manuscript for submission to *ACS Earth and Space Chemistry*

334 **Supporting Information.** Instrument modifications and schematic; oxidation details; modeling  
335 details; reaction mechanisms.

### 336 **Corresponding Author**

337 \*Sarah S. Petters, spetters@unc.edu.

### 338 **Present Addresses**

339 †now at Institut de Recherches sur la Catalyse et l'Environnement de Lyon (IRCELYON), CNRS, and  
340 Université Lyon 1, Villeurbanne, 69626 France.

### 341 **Funding Sources**

342 This project was funded by the U.S. National Science Foundation Postdoctoral Fellowship under  
343 Award #AGS-1624696. REHM was supported by the U.K. Engineering and Physical Sciences  
344 Research Council, grant number EP/N025245/1. We thank Sara Duncan for assistance with some  
345 of the experiments.

## 346 **5. References**

- 347 (1) Mao, J.; Carlton, A.; Cohen, R. C.; Brune, W. H.; Brown, S. S.; Wolfe, G. M.; Jimenez, J.  
348 L.; Pye, H. O. T.; Lee Ng, N.; Xu, L.; et al. Southeast Atmosphere Studies: Learning from  
349 Model-Observation Syntheses. *Atmos. Chem. Phys.* **2018**, *18* (4), 2615–2651. doi:  
350 10.5194/acp-18-2615-2018.
- 351 (2) Chan Miller, C.; Jacob, D. J.; Marais, E. A.; Yu, K.; Travis, K. R.; Kim, P. S.; Fisher, J. A.;  
352 Zhu, L.; Wolfe, G. M.; Hanisco, T. F.; et al. Glyoxal Yield from Isoprene Oxidation and  
353 Relation to Formaldehyde: Chemical Mechanism, Constraints from SENEX Aircraft  
354 Observations, and Interpretation of OMI Satellite Data. *Atmos. Chem. Phys.* **2017**, *17* (14),  
355 8725–8738. doi: 10.5194/acp-17-8725-2017.
- 356 (3) Marais, E. A.; Jacob, D. J.; Jimenez, J. L.; Campuzano-Jost, P.; Day, D. A.; Hu, W.;  
357 Krechmer, J.; Zhu, L.; Kim, P. S.; Miller, C. C.; et al. Aqueous-Phase Mechanism for  
358 Secondary Organic Aerosol Formation from Isoprene: Application to the Southeast United  
359 States and Co-Benefit of SO<sub>2</sub> Emission Controls. *Atmos. Chem. Phys.* **2016**, *16* (3), 1603–  
360 1618. doi: 10.5194/acp-16-1603-2016.

Manuscript for submission to *ACS Earth and Space Chemistry*

- 1  
2  
3 361 (4) Ervens, B.; Turpin, B. J.; Weber, R. J. Secondary Organic Aerosol Formation in Cloud  
4 362 Droplets and Aqueous Particles (AqSOA): A Review of Laboratory, Field and Model  
5 363 Studies. *Atmos. Chem. Phys.* **2011**, *11* (21), 11069–11102. doi: 10.5194/acp-11-11069-  
6 364 2011.
- 8  
9 365 (5) Blando, J. D.; Turpin, B. J. Secondary Organic Aerosol Formation in Cloud and Fog  
10 366 Droplets: A Literature Evaluation of Plausibility. *Atmos. Environ.* **2000**, *34* (10), 1623–  
11 367 1632. doi: 10.1016/S1352-2310(99)00392-1.
- 13  
14 368 (6) Budisulistiorini, S. H.; Canagaratna, M. R.; Croteau, P. L.; Marth, W. J.; Baumann, K.;  
15 369 Edgerton, E. S.; Shaw, S. L.; Knipping, E. M.; Worsnop, D. R.; Jayne, J. T.; et al. Real-  
16 370 Time Continuous Characterization of Secondary Organic Aerosol Derived from Isoprene  
17 371 Epoxydiols in Downtown Atlanta, Georgia, Using the Aerodyne Aerosol Chemical  
18 372 Speciation Monitor. *Environ. Sci. Technol.* **2013**, *47* (11), 5686–5694. doi: 10.1021/  
19 373 es400023n.
- 21  
22 374 (7) McVay, R.; Ervens, B. A Microphysical Parameterization of AqSOA and Sulfate Formation  
23 375 in Clouds. *Geophys. Res. Lett.* **2017**, *44* (14), 7500–7509. doi: 10.1002/2017GL074233.
- 25  
26 376 (8) Woo, J. L.; McNeill, V. F. SimpleGAMMA v1.0 – a Reduced Model of Secondary Organic  
27 377 Aerosol Formation in the Aqueous Aerosol Phase (AaSOA). *Geosci. Model. Dev.* **2015**, *8*  
28 378 (6), 1821–1829. doi: 10.5194/gmd-8-1821-2015.
- 30  
31 379 (9) Heald, C. L.; Coe, H.; Jimenez, J. L.; Weber, R. J.; Bahreini, R.; Middlebrook, A. M.;  
32 380 Russell, L. M.; Jolleys, M.; Fu, T.-M.; Allan, J. D.; et al. Exploring the Vertical Profile of  
33 381 Atmospheric Organic Aerosol: Comparing 17 Aircraft Field Campaigns with a Global  
34 382 Model. *Atmos. Chem. Phys.* **2011**, *11* (24), 12673–12696. doi: 10.5194/acp-11-12673-2011.
- 35  
36 383 (10) Carlton, A. G.; Turpin, B. J.; Altieri, K. E.; Seitzinger, S. P.; Mathur, R.; Roselle, S. J.;  
37 384 Weber, R. J. CMAQ Model Performance Enhanced When In-Cloud Secondary Organic  
38 385 Aerosol Is Included: Comparisons of Organic Carbon Predictions with Measurements.  
39 386 *Environ. Sci. Technol.* **2008**, *42* (23), 8798–8802. doi: 10.1021/es801192n.
- 41  
42 387 (11) Fu, T.-M.; Jacob, D. J.; Wittrock, F.; Burrows, J. P.; Vrekoussis, M.; Henze, D. K. Global  
43 388 Budgets of Atmospheric Glyoxal and Methylglyoxal, and Implications for Formation of  
44 389 Secondary Organic Aerosols. *J. Geophys. Res. Atmospheres* **2008**, *113*, D15303. doi:  
45 390 10.1029/2007JD009505.
- 46  
47 391 (12) Ortiz-Montalvo, D.; Häkkinen, S. A. K.; Schwier, A. N.; Lim, Y. B.; McNeill, V. F.; Turpin,  
48 392 B. J. Ammonium Addition (and Aerosol pH) Has a Dramatic Impact on the Volatility and  
49 393 Yield of Glyoxal Secondary Organic Aerosol. *Environ. Sci. Technol.* **2014**, *48* (1), 255–262.  
50 394 doi: 10.1021/es4035667.
- 52  
53 395 (13) Carlton, A. G.; Turpin, B. J.; Altieri, K. E.; Seitzinger, S.; Reff, A.; Lim, H.-J.; Ervens, B.  
54 396 Atmospheric Oxalic Acid and SOA Production from Glyoxal: Results of Aqueous

Manuscript for submission to *ACS Earth and Space Chemistry*

- 397 Photooxidation Experiments. *Atmos. Environ.* **2007**, *41* (35), 7588–7602. doi: 10.1016/  
398 j.atmosenv.2007.05.035.
- (14) Tan, Y.; Perri, M. J.; Seitzinger, S. P.; Turpin, B. J. Effects of Precursor Concentration and  
Acidic Sulfate in Aqueous Glyoxal–OH Radical Oxidation and Implications for Secondary  
Organic Aerosol. *Environ. Sci. Technol.* **2009**, *43* (21), 8105–8112. doi: 10.1021/es901742f.
- (15) Perri, M. J.; Seitzinger, S.; Turpin, B. J. Secondary Organic Aerosol Production from  
Aqueous Photooxidation of Glycolaldehyde: Laboratory Experiments. *Atmos. Environ.*  
**2009**, *43* (8), 1487–1497. doi: 10.1016/j.atmosenv.2008.11.037.
- (16) Ortiz-Montalvo, D.; Lim, Y. B.; Perri, M. J.; Seitzinger, S. P.; Turpin, B. J. Volatility and  
Yield of Glycolaldehyde SOA Formed through Aqueous Photochemistry and Droplet  
Evaporation. *Aerosol Sci. Technol.* **2012**, *46* (9), 1002–1014. doi: 10.1080/  
02786826.2012.686676.
- (17) Michaud, V.; El Haddad, I.; Yao Liu; Sellegri, K.; Laj, P.; Villani, P.; Picard, D.; Marchand,  
N.; Monod, A. In-Cloud Processes of Methacrolein under Simulated Conditions – Part 3:  
Hygroscopic and Volatility Properties of the Formed Secondary Organic Aerosol. *Atmos.*  
*Chem. Phys.* **2009**, *9* (14), 5119–5130. doi: 10.5194/acp-9-5119-2009.
- (18) Tan, Y.; Lim, Y. B.; Altieri, K. E.; Seitzinger, S. P.; Turpin, B. J. Mechanisms Leading to  
Oligomers and SOA through Aqueous Photooxidation: Insights from OH Radical Oxidation  
of Acetic Acid and Methylglyoxal. *Atmos. Chem. Phys.* **2012**, *12* (2), 801–813. doi:  
10.5194/acp-12-801-2012.
- (19) Tan, Y.; Carlton, A. G.; Seitzinger, S. P.; Turpin, B. J. SOA from Methylglyoxal in Clouds  
and Wet Aerosols: Measurement and Prediction of Key Products. *Atmos. Environ.* **2010**, *44*  
(39), 5218–5226. doi: 10.1016/j.atmosenv.2010.08.045.
- (20) Lim, Y. B.; Turpin, B. J. Laboratory Evidence of Organic Peroxide and Peroxyhemiacetal  
Formation in the Aqueous Phase and Implications for Aqueous OH. *Atmos. Chem. Phys.*  
**2015**, *15* (22), 12867–12877. doi: 10.5194/acp-15-12867-2015.
- (21) Ortiz-Montalvo, D.; Schwier, A. N.; Lim, Y. B.; McNeill, V. F.; Turpin, B. J. Volatility of  
Methylglyoxal Cloud SOA Formed through OH Radical Oxidation and Droplet  
Evaporation. *Atmos. Environ.* **2016**, *130*, 145–152. doi: 10.1016/j.atmosenv.2015.12.013.
- (22) Renard, P.; Reed Harris, A. E.; Rapf, R. J.; Ravier, S.; Demelas, C.; Coulomb, B.; Quivet,  
E.; Vaida, V.; Monod, A. Aqueous Phase Oligomerization of Methyl Vinyl Ketone by  
Atmospheric Radical Reactions. *J. Phys. Chem. C* **2014**, *118* (50), 29421–29430. doi:  
10.1021/jp5065598.
- (23) Yu, L.; Smith, J.; Laskin, A.; George, K. M.; Anastasio, C.; Laskin, J.; Dillner, A. M.;  
Zhang, Q. Molecular Transformations of Phenolic SOA during Photochemical Aging in the  
Aqueous Phase: Competition among Oligomerization, Functionalization, and

Manuscript for submission to *ACS Earth and Space Chemistry*

- 433 Fragmentation. *Atmos. Chem. Phys.* **2016**, *16* (7), 4511–4527. doi: 10.5194/acp-16-4511-  
434 2016.
- 435 (24) Altieri, K. E.; Carlton, A. G.; Lim, H.-J.; Turpin, B. J.; Seitzinger, S. P. Evidence for  
436 Oligomer Formation in Clouds: Reactions of Isoprene Oxidation Products. *Environ. Sci.*  
437 *Technol.* **2006**, *40* (16), 4956–4960. doi: 10.1021/es052170n.
- 438 (25) Carlton, A. G.; Turpin, B. J.; Lim, H.-J.; Altieri, K. E.; Seitzinger, S. Link between Isoprene  
439 and Secondary Organic Aerosol (SOA): Pyruvic Acid Oxidation Yields Low Volatility  
440 Organic Acids in Clouds. *Geophys. Res. Lett.* **2006**, *33* (6). doi: 10.1029/2005GL025374.
- 441 (26) Griffith, E. C.; Carpenter, B. K.; Shoemaker, R. K.; Vaida, V. Photochemistry of Aqueous  
442 Pyruvic Acid. *Proc. Natl. Acad. Sci. USA* **2013**, *110* (29), 11714. doi: 10.1073/  
443 pnas.1303206110.
- 444 (27) Bernard, F.; Ciuraru, R.; Boréave, A.; George, C. Photosensitized Formation of Secondary  
445 Organic Aerosols above the Air/Water Interface. *Environ. Sci. Technol.* **2016**, *50* (16),  
446 8678–8686. doi: 10.1021/acs.est.6b03520.
- 447 (28) Rapf, R. J.; Perkins, R. J.; Dooley, M. R.; Kroll, J. A.; Carpenter, B. K.; Vaida, V.  
448 Environmental Processing of Lipids Driven by Aqueous Photochemistry of  $\alpha$ -Keto Acids.  
449 *ACS Cent. Sci.* **2018**, *4* (5), 624–630. doi: 10.1021/acscentsci.8b00124.
- 450 (29) Galloway, M. M.; Powelson, M. H.; Sedehi, N.; Wood, S. E.; Millage, K. D.; Kononenko,  
451 J. A.; Rynaski, A. D.; De Haan, D. O. Secondary Organic Aerosol Formation during  
452 Evaporation of Droplets Containing Atmospheric Aldehydes, Amines, and Ammonium  
453 Sulfate. *Environ. Sci. Technol.* **2014**, *48* (24), 14417–14425. doi: 10.1021/es5044479.
- 454 (30) De Haan, D. O.; Corrigan, A. L.; Tolbert, M. A.; Jimenez, J. L.; Wood, S. E.; Turley, J. J.  
455 Secondary Organic Aerosol Formation by Self-Reactions of Methylglyoxal and Glyoxal in  
456 Evaporating Droplets. *Environ. Sci. Technol.* **2009**, *43* (21), 8184–8190. doi:  
457 10.1021/es902152t.
- 458 (31) Surratt, J. D.; Chan, A. W. H.; Eddingsaas, N. C.; Chan, M.; Loza, C. L.; Kwan, A. J.;  
459 Hersey, S. P.; Flagan, R. C.; Wennberg, P. O.; Seinfeld, J. H. Reactive Intermediates  
460 Revealed in Secondary Organic Aerosol Formation from Isoprene. *Proc. Natl. Acad. Sci.*  
461 *USA* **2010**, *107* (15), 6640–6645. doi: 10.1073/pnas.0911114107.
- 462 (32) Lee, A. K. Y.; Zhao, R.; Li, R.; Liggio, J.; Li, S.-M.; Abbatt, J. P. D. Formation of Light  
463 Absorbing Organo-Nitrogen Species from Evaporation of Droplets Containing Glyoxal and  
464 Ammonium Sulfate. *Environ. Sci. Technol.* **2013**, *47* (22), 12819–12826. doi: 10.1021/  
465 es402687w.
- 466 (33) Ervens, B. Progress and Problems in Modeling Chemical Processing in Cloud Droplets and  
467 Wet Aerosol Particles. In *Multiphase Environmental Chemistry in the Atmosphere*; ACS

Manuscript for submission to *ACS Earth and Space Chemistry*

- 468 Symposium Series; American Chemical Society, 2018; Vol. 1299, pp 327–345. doi:  
469 10.1021/bk-2018-1299.ch016.
- 470 (34) Donahue, N. M.; Kroll, J. H.; Pandis, S. N.; Robinson, A. L. A Two-Dimensional Volatility  
471 Basis Set – Part 2: Diagnostics of Organic-Aerosol Evolution. *Atmos. Chem. Phys.* **2012**, *12*  
472 (2), 615–634. doi: 10.5194/acp-12-615-2012.
- 473 (35) Loeffler, K. W.; Koehler, C. A.; Paul, N. M.; De Haan, D. O. Oligomer Formation in  
474 Evaporating Aqueous Glyoxal and Methyl Glyoxal Solutions. *Environ. Sci. Technol.* **2006**,  
475 *40* (20), 6318–6323. doi: 10.1021/es060810w.
- 476 (36) Barsanti, K. C.; Kroll, J. H.; Thornton, J. A. Formation of Low-Volatility Organic  
477 Compounds in the Atmosphere: Recent Advancements and Insights. *J. Phys. Chem. Lett.*  
478 **2017**, *8* (7), 1503–1511. doi: 10.1021/acs.jpcclett.6b02969.
- 479 (37) Girod, M.; Moyano, E.; Campbell, D. I.; Cooks, R. G. Accelerated Bimolecular Reactions  
480 in Microdroplets Studied by Desorption Electrospray Ionization Mass Spectrometry. *Chem.*  
481 *Sci.* **2011**, *2* (3), 501–510. doi: 10.1039/C0SC00416B.
- 482 (38) Marsh, B. M.; Iyer, K.; Cooks, R. G. Reaction Acceleration in Electrospray Droplets: Size,  
483 Distance, and Surfactant Effects. *J. Am. Soc. Mass Spectrom.* **2019**. doi: 10.1007/s13361-  
484 019-02264-w.
- 485 (39) Bain, R. M.; Pulliam, C. J.; They, F.; Cooks, R. G. Accelerated Chemical Reactions and  
486 Organic Synthesis in Leidenfrost Droplets. *Angew. Chem. Int. Ed.* **2016**, *55* (35), 10478–  
487 10482. doi: 10.1002/anie.201605899.
- 488 (40) Badu-Tawiah, A. K.; Campbell, D. I.; Cooks, R. G. Reactions of Microsolvated Organic  
489 Compounds at Ambient Surfaces: Droplet Velocity, Charge State, and Solvent Effects. *J.*  
490 *Am. Soc. Mass Spectrom.* **2012**, *23* (6), 1077–1084. doi: 10.1007/s13361-012-0365-3.
- 491 (41) Nguyen, T. B.; Lee, P. B.; Updyke, K. M.; Bones, D. L.; Laskin, J.; Laskin, A.; Nizkorodov,  
492 S. A. Formation of Nitrogen- and Sulfur-Containing Light-Absorbing Compounds  
493 Accelerated by Evaporation of Water from Secondary Organic Aerosols. *J. Geophys. Res.*  
494 *Atmos.* **2012**, *117* (D1). doi: 10.1029/2011JD016944.
- 495 (42) Li, Y.; Yan, X.; Cooks, R. G. The Role of the Interface in Thin Film and Droplet Accelerated  
496 Reactions Studied by Competitive Substituent Effects. *Angew. Chem. Int. Ed.* **2016**, *55* (10),  
497 3433–3437. doi: 10.1002/anie.201511352.
- 498 (43) Zhong, J.; Kumar, M.; Francisco, J. S.; Zeng, X. C. Insight into Chemistry on Cloud/Aerosol  
499 Water Surfaces. *Acc. Chem. Res.* **2018**, *51* (5), 1229–1237. doi: 10.1021/  
500 acs.accounts.8b00051.



Manuscript for submission to *ACS Earth and Space Chemistry*

- 1  
2  
3 501 (44) Eugene, A. J.; Pillar, E. A.; Colussi, A. J.; Guzman, M. I. Enhanced Acidity of Acetic and  
4 502 Pyruvic Acids on the Surface of Water. *Langmuir* **2018**, *34* (31), 9307–9313. doi:  
5 503 10.1021/acs.langmuir.8b01606.  
6  
7  
8 504 (45) Narayan, S.; Muldoon, J.; Finn, M. G.; Fokin, V. V.; Kolb, H. C.; Sharpless, K. B. “On  
9 505 Water”: Unique Reactivity of Organic Compounds in Aqueous Suspension. *Angew. Chem.*  
10 506 *Int. Ed.* **2005**, *44* (21), 3275–3279. doi: 10.1002/anie.200462883.  
11  
12 507 (46) Donaldson, D. J.; Vaida, V. The Influence of Organic Films at the Air–Aqueous Boundary  
13 508 on Atmospheric Processes. *Chem. Rev.* **2006**, *106* (4), 1445–1461. doi: 10.1021/cr040367c.  
14  
15  
16 509 (47) Nishino, N.; Hollingsworth, S. A.; Stern, A. C.; Roeselová, M.; Tobias, D. J.; Finlayson-  
17 510 Pitts, B. J. Interactions of Gaseous HNO<sub>3</sub> and Water with Individual and Mixed Alkyl Self-  
18 511 Assembled Monolayers at Room Temperature. *Phys. Chem. Chem. Phys.* **2014**, *16* (6),  
19 512 2358–2367. doi: 10.1039/C3CP54118E.  
20  
21  
22 513 (48) Wingen, L. M.; Moskun, A. C.; Johnson, S. N.; Thomas, J. L.; Roeselová, M.; Tobias, D.  
23 514 J.; Kleinman, M. T.; Finlayson-Pitts, B. J. Enhanced Surface Photochemistry in Chloride–  
24 515 Nitrate Ion Mixtures. *Phys. Chem. Chem. Phys.* **2008**, *10* (37), 5668–5677. doi:  
25 516 10.1039/B806613B.  
26  
27  
28 517 (49) Stefan, M. I.; Bolton, J. R. Reinvestigation of the Acetone Degradation Mechanism in Dilute  
29 518 Aqueous Solution by the UV/H<sub>2</sub>O<sub>2</sub> Process. *Environ. Sci. Technol.* **1999**, *33* (6), 870–873.  
30 519 doi: 10.1021/es9808548.  
31  
32 520 (50) Kawamura, K.; Tachibana, E.; Okuzawa, K.; Aggarwal, S. G.; Kanaya, Y.; Wang, Z. F.  
33 521 High Abundances of Water-Soluble Dicarboxylic Acids, Ketocarboxylic Acids and  $\alpha$ -  
34 522 Dicarboxyls in the Mountaintop Aerosols over the North China Plain during Wheat Burning  
35 523 Season. *Atmos. Chem. Phys.* **2013**, *13* (16), 8285–8302. doi: 10.5194/acp-13-8285-2013.  
36  
37  
38 524 (51) Talbot, R. W.; Andreae, M. O.; Berresheim, H.; Jacob, D. J.; Beecher, K. M. Sources and  
39 525 Sinks of Formic, Acetic, and Pyruvic Acids over Central Amazonia: 2. Wet Season. *J.*  
40 526 *Geophys. Res. Atmos.* **1990**, *95*, 16799–16811. doi: 10.1029/JD095iD10p16799.  
41  
42  
43 527 (52) Praplan, A. P.; Hegyi-Gaeggeler, K.; Barmet, P.; Pfaffenberger, L.; Dommen, J.;  
44 528 Baltensperger, U. Online Measurements of Water-Soluble Organic Acids in the Gas and  
45 529 Aerosol Phase from the Photooxidation of 1,3,5-Trimethylbenzene. *Atmos. Chem. Phys.*  
46 530 **2014**, *14* (16), 8665–8677. doi: 10.5194/acp-14-8665-2014.  
47  
48  
49 531 (53) Mattila, J. M.; Brophy, P.; Kirkland, J.; Hall, S.; Ullmann, K.; Fischer, E. V.; Brown, S.;  
50 532 McDuffie, E.; Tevlin, A.; Farmer, D. K. Tropospheric Sources and Sinks of Gas-Phase  
51 533 Acids in the Colorado Front Range. *Atmos. Chem. Phys.* **2018**, *18* (16), 12315–12327. doi:  
52 534 10.5194/acp-18-12315-2018.  
53  
54  
55  
56  
57  
58  
59  
60

Manuscript for submission to *ACS Earth and Space Chemistry*

- 1  
2  
3 535 (54) Andino, J. M.; Smith, J. N.; Flagan, R. C.; Goddard, W. A.; Seinfeld, J. H. Mechanism of  
4 536 Atmospheric Photooxidation of Aromatics: A Theoretical Study. *J. Phys. Chem.* **1996**, *100*  
5 537 (26), 10967–10980. doi: 10.1021/jp9529351.  
6  
7  
8 538 (55) Veres, P.; Roberts, J. M.; Burling, I. R.; Warneke, C.; de Gouw, J.; Yokelson, R. J.  
9 539 Measurements of Gas-Phase Inorganic and Organic Acids from Biomass Fires by Negative-  
10 540 Ion Proton-Transfer Chemical-Ionization Mass Spectrometry. *J. Geophys. Res. Atmos.*  
11 541 **2010**, *115* (D23). doi: 10.1029/2010JD014033.  
12  
13  
14 542 (56) Reed Harris, A. E.; Pajunoja, A.; Cazaunau, M.; Gratien, A.; Pangui, E.; Monod, A.;  
15 543 Griffith, E. C.; Virtanen, A.; Doussin, J.-F.; Vaida, V. Multiphase Photochemistry of  
16 544 Pyruvic Acid under Atmospheric Conditions. *J. Phys. Chem. A* **2017**, *121* (18), 3327–3339.  
17 545 doi: 10.1021/acs.jpca.7b01107.  
18  
19  
20 546 (57) Andreae, M. O.; Talbot, R. W.; Li, S.-M. Atmospheric Measurements of Pyruvic and Formic  
21 547 Acid. *J. Geophys. Res. Atmos.* **1987**, *92*, 6635–6641. doi: 10.1029/JD092iD06p06635.  
22  
23 548 (58) Guzmán, M. I.; Colussi, A. J.; Hoffmann, M. R. Photoinduced Oligomerization of Aqueous  
24 549 Pyruvic Acid. *J. Phys. Chem. A* **2006**, *110* (10), 3619–3626. doi: 10.1021/jp056097z.  
25  
26  
27 550 (59) Schaefer, T.; Schindelka, J.; Hoffmann, D.; Herrmann, H. Laboratory Kinetic and  
28 551 Mechanistic Studies on the OH-Initiated Oxidation of Acetone in Aqueous Solution. *J.*  
29 552 *Phys. Chem. A* **2012**, *116* (24), 6317–6326. doi: 10.1021/jp2120753.  
30  
31 553 (60) Healy, R. M.; Wenger, J. C.; Metzger, A.; Duplissy, J.; Kalberer, M.; Dommen, J.  
32 554 Gas/Particle Partitioning of Carbonyls in the Photooxidation of Isoprene and 1,3,5-  
33 555 Trimethylbenzene. *Atmos. Chem. Phys.* **2008**, *8* (12), 3215–3230. doi: 10.5194/acp-8-3215-  
34 556 2008.  
35  
36  
37 557 (61) Berglund, R. N.; Liu, B. Y. H. Generation of Monodisperse Aerosol Standards. *Environ.*  
38 558 *Sci. Technol.* **1973**, *7* (2), 147–153. doi: 10.1021/es60074a001.  
39  
40  
41 559 (62) Werner, F.; Ditas, F.; Siebert, H.; Simmel, M.; Wehner, B.; Pilewskie, P.; Schmeissner, T.;  
42 560 Shaw, R. A.; Hartmann, S.; Wex, H.; et al. Twomey Effect Observed from Collocated  
43 561 Microphysical and Remote Sensing Measurements over Shallow Cumulus. *J. Geophys. Res.*  
44 562 *Atmos.* **2014**, *119* (3), 1534–1545. doi: 10.1002/2013JD020131.  
45  
46  
47 563 (63) Barr, E. B.; Carpenter, R. L.; Newton, G. J. Improved Liquid Feed System for the Berglund-  
48 564 Liu Vibrating Orifice Monodisperse Aerosol Generator. *Environ. Sci. Technol.* **1984**, *18* (9),  
49 565 721–723. doi: 10.1021/es00127a016.  
50  
51 566 (64) Devarakonda, V.; Ray, A. K.; Kaiser, T.; Schweiger, G. Vibrating Orifice Droplet Generator  
52 567 for Studying Fast Processes Associated with Microdroplets. *Aerosol Sci. Technol.* **1998**, *28*  
53 568 (6), 531–547. doi: 10.1080/02786829808965544.  
54  
55  
56  
57  
58  
59  
60

Manuscript for submission to *ACS Earth and Space Chemistry*

- 1  
2  
3 569 (65) Mavrogiannis, N.; Ibo, M.; Fu, X.; Crivellari, F.; Gagnon, Z. Microfluidics Made Easy: A  
4 570 Robust Low-Cost Constant Pressure Flow Controller for Engineers and Cell Biologists.  
5 571 *Biomicrofluidics* **2016**, *10* (3), 034107. doi: 10.1063/1.4950753.
- 7  
8 572 (66) Petters, M. D.; Kreidenweis, S. M.; Prenni, A. J.; Sullivan, R. C.; Carrico, C. M.; Koehler,  
9 573 K. A.; Ziemann, P. J. Role of Molecular Size in Cloud Droplet Activation. *Geophys. Res.*  
10 574 *Lett.* **2009**, *36* (22), L22801. doi: 10.1029/2009GL040131.
- 12  
13 575 (67) Petters, S. S.; Pagonis, D.; Claflin, M. S.; Levin, E. J. T.; Petters, M. D.; Ziemann, P. J.;  
14 576 Kreidenweis, S. M. Hygroscopicity of Organic Compounds as a Function of Carbon Chain  
15 577 Length and Carboxyl, Hydroperoxy, and Carbonyl Functional Groups. *J. Phys. Chem. A*  
16 578 **2017**, *121* (27), 5164–5174. doi: 10.1021/acs.jpca.7b04114.
- 18  
19 579 (68) Davies, J. F.; Haddrell, A. E.; Reid, J. P. Time-Resolved Measurements of the Evaporation  
20 580 of Volatile Components from Single Aerosol Droplets. *Aerosol Sci. Technol.* **2012**, *46* (6),  
21 581 666–677. doi: 10.1080/02786826.2011.652750.
- 23  
24 582 (69) Rovelli, G.; Miles, R. E. H.; Reid, J. P.; Clegg, S. L. Accurate Measurements of Aerosol  
25 583 Hygroscopic Growth over a Wide Range in Relative Humidity. *J. Phys. Chem. A* **2016**, *120*  
26 584 (25), 4376–4388. doi: 10.1021/acs.jpca.6b04194.
- 28  
29 585 (70) Su, Y.-Y.; Marsh, A.; Haddrell, A. E.; Li, Z.-M.; Reid, J. P. Evaporation Kinetics of Polyol  
30 586 Droplets: Determination of Evaporation Coefficients and Diffusion Constants. *J. Geophys.*  
31 587 *Res. Atmos.* **2017**, *122* (22), 12,317–12,334. doi: 10.1002/2017JD027111.
- 32  
33 588 (71) Dawson, K. W.; Petters, M. D.; Meskhidze, N.; Petters, S. S.; Kreidenweis, S. M.  
34 589 Hygroscopic Growth and Cloud Droplet Activation of Xanthan Gum as a Proxy for Marine  
35 590 Hydrogels. *J. Geophys. Res. Atmos.* **2016**, *121* (19), 11803–11818. doi: 10.1002/  
36 591 2016JD025143.
- 38  
39 592 (72) Tomaz, S.; Cui, T.; Chen, Y.; Sexton, K. G.; Roberts, J. M.; Warneke, C.; Yokelson, R. J.;  
40 593 Surratt, J. D.; Turpin, B. J. Photochemical Cloud Processing of Primary Wildfire Emissions  
41 594 as a Potential Source of Secondary Organic Aerosol. *Environ. Sci. Technol.* **2018**, *52* (19),  
42 595 11027–11037. doi: 10.1021/acs.est.8b03293.
- 44  
45 596 (73) van Pinxteren, D.; Fomba, K. W.; Mertes, S.; Müller, K.; Spindler, G.; Schneider, J.; Lee,  
46 597 T.; Collett, J. L.; Herrmann, H. Cloud Water Composition during HCCT-2010: Scavenging  
47 598 Efficiencies, Solute Concentrations, and Droplet Size Dependence of Inorganic Ions and  
48 599 Dissolved Organic Carbon. *Atmospheric Chem. Phys.* **2016**, *16* (5), 3185–3205. doi:  
49 600 10.5194/acp-16-3185-2016.
- 51  
52 601 (74) Deguillaume, L.; Charbouillot, T.; Joly, M.; Vaïtilingom, M.; Parazols, M.; Marinoni, A.;  
53 602 Amato, P.; Delort, A.-M.; Vinatier, V.; Flossmann, A.; et al. Classification of Clouds  
54 603 Sampled at the Puy de Dôme (France) Based on 10 Yr of Monitoring of Their  
55 604 Physicochemical Properties. *Atmos. Chem. Phys.* **2014**, *14* (3), 1485–1506. doi:  
56 605 10.5194/acp-14-1485-2014.

Manuscript for submission to *ACS Earth and Space Chemistry*

- 606 (75) Lim, Y. B.; Tan, Y.; Turpin, B. J. Chemical Insights, Explicit Chemistry, and Yields of  
607 Secondary Organic Aerosol from OH Radical Oxidation of Methylglyoxal and Glyoxal in  
608 the Aqueous Phase. *Atmos. Chem. Phys.* **2013**, *13* (17), 8651–8667. doi: 10.5194/acp-13-  
609 8651-2013.
- 610 (76) Herrmann, H.; Hoffmann, D.; Schaefer, T.; Brüner, P.; Tilgner, A. Tropospheric Aqueous-  
611 Phase Free-Radical Chemistry: Radical Sources, Spectra, Reaction Kinetics and Prediction  
612 Tools. *Chem. Phys. Phys. Chem.* **2010**, *11* (18), 3796–3822. doi: 10.1002/cphc.201000533.
- 613 (77) Arakaki, T.; Anastasio, C.; Kuroki, Y.; Nakajima, H.; Okada, K.; Kotani, Y.; Handa, D.;  
614 Azechi, S.; Kimura, T.; Tsuchi, A.; et al. A General Scavenging Rate Constant for  
615 Reaction of Hydroxyl Radical with Organic Carbon in Atmospheric Waters. *Environ. Sci.*  
616 *Technol.* **2013**, *47* (15), 8196–8203. doi: 10.1021/es401927b.
- 617 (78) Ahn, K.-H.; Liu, B. Y. H. Particle Activation and Droplet Growth Processes in  
618 Condensation Nucleus Counter—I. Theoretical Background. *J. Aerosol Sci.* **1990**, *21* (2),  
619 249–261. doi: 10.1016/0021-8502(90)90008-L.
- 620 (79) Bilde, M.; Svenningsson, B.; Mønster, J.; Rosenørn, T. Even–Odd Alternation of  
621 Evaporation Rates and Vapor Pressures of C3–C9 Dicarboxylic Acid Aerosols. *Environ.*  
622 *Sci. Technol.* **2003**, *37* (7), 1371–1378. doi: 10.1021/es0201810.
- 623 (80) Hinds, W. C. *Aerosol Technology: Properties, Behavior, and Measurement of Airborne*  
624 *Particles*, 2nd ed.; John Wiley and Sons: New York, 1999.
- 625 (81) Davis, E. J.; Ray, A. K. Submicron Droplet Evaporation in the Continuum and Non-  
626 Continuum Regimes. *J. Aerosol Sci.* **1978**, *9* (5), 411–422. doi: 10.1016/0021-  
627 8502(78)90003-4.
- 628 (82) Hirschfelder, J. O.; Curtiss, C. F.; Bird, R. B. *Molecular Theory of Gases and Liquids*;  
629 Wiley, 1967.
- 630 (83) Lim, H.-J.; Carlton, A. G.; Turpin, B. J. Isoprene Forms Secondary Organic Aerosol  
631 Through Cloud Processing: Model Simulations. *Environ. Sci. Technol.* **2005**, *39* (12), 4441–  
632 4446. doi: 10.1021/es048039h.
- 633 (84) Suda, S. R.; Petters, M. D. Accurate Determination of Aerosol Activity Coefficients at  
634 Relative Humidities up to 99% Using the Hygroscopicity Tandem Differential Mobility  
635 Analyzer Technique. *Aerosol Sci. Technol.* **2013**, *47* (9), 991–1000. doi: 10.1080/  
636 02786826.2013.807906.
- 637 (85) Suda, S. R.; Petters, M. D.; Matsunaga, A.; Sullivan, R. C.; Ziemann, P. J.; Kreidenweis, S.  
638 M. Hygroscopicity Frequency Distributions of Secondary Organic Aerosols. *J. Geophys.*  
639 *Res. Atmos.* **2012**, *117*, D04207. doi: 10.1029/2011JD016823.

Manuscript for submission to *ACS Earth and Space Chemistry*

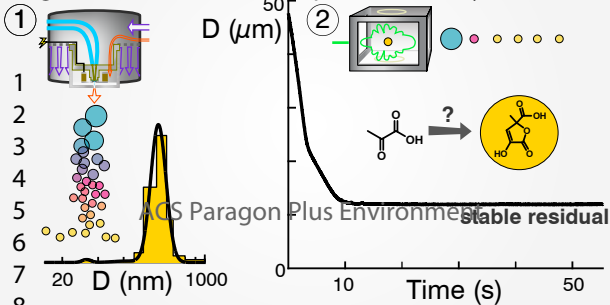
- 640 (86) Pocker, Y.; Meany, J. E.; Nist, B. J.; Zadorojny, C. Reversible Hydration of Pyruvic Acid.  
641 I. Equilibrium Studies. *J. Phys. Chem.* **1969**, *73* (9), 2879–2882. doi: 10.1021/j100843a015.
- 642 (87) Liggio, J.; Li, S.-M.; McLaren, R. Heterogeneous Reactions of Glyoxal on Particulate  
643 Matter: Identification of Acetals and Sulfate Esters. *Environ. Sci. Technol.* **2005**, *39* (6),  
644 1532–1541. doi: 10.1021/es048375y.
- 645 (88) Rapf, R. J.; Dooley, M. R.; Kappes, K.; Perkins, R. J.; Vaida, V. PH Dependence of the  
646 Aqueous Photochemistry of  $\hat{\text{I}}\pm$ -Keto Acids. *J. Phys. Chem. A* **2017**, *121* (44), 8368–8379.  
647 doi: 10.1021/acs.jpca.7b08192.
- 648 (89) Perkins, R. J.; Shoemaker, R. K.; Carpenter, B. K.; Vaida, V. Chemical Equilibria and  
649 Kinetics in Aqueous Solutions of Zymonic Acid. *J. Phys. Chem. A* **2016**, *120* (51), 10096–  
650 10107. doi: 10.1021/acs.jpca.6b10526.
- 651 (90) Otto, T.; Stieger, B.; Mettke, P.; Herrmann, H. Tropospheric Aqueous-Phase Oxidation of  
652 Isoprene-Derived Dihydroxycarbonyl Compounds. *J. Phys. Chem. A* **2017**, *121* (34), 6460–  
653 6470. doi: 10.1021/acs.jpca.7b05879.
- 654 (91) Mellouki, A.; Mu, Y. On the Atmospheric Degradation of Pyruvic Acid in the Gas Phase.  
655 *Atmos. Photochem.* **2003**, *157* (2), 295–300. doi: 10.1016/S1010-6030(03)00070-4.
- 656 (92) Sander, R. Compilation of Henry's Law Constants (Version 4.0) for Water as Solvent.  
657 *Atmos. Chem. Phys.* **2015**, *15* (8), 4399–4981. doi: 10.5194/acp-15-4399-2015.
- 658 (93) Epstein, S. A.; Nizkorodov, S. A. A Comparison of the Chemical Sinks of Atmospheric  
659 Organics in the Gas and Aqueous Phase. *Atmos. Chem. Phys.* **2012**, *12* (17), 8205–8222.  
660 doi: 10.5194/acp-12-8205-2012.
- 661 (94) Herrmann, H.; Schaefer, T.; Tilgner, A.; Styler, S. A.; Weller, C.; Teich, M.; Otto, T.  
662 Tropospheric Aqueous-Phase Chemistry: Kinetics, Mechanisms, and Its Coupling to a  
663 Changing Gas Phase. *Chem. Rev.* **2015**, *115* (10), 4259–4334. doi: 10.1021/cr500447k.
- 664 (95) Stull, D. R. Inorganic Compounds. *Ind. Eng. Chem.* **1947**, *39* (4), 540–550. doi:  
665 10.1021/ie50448a023.
- 666 (96) Emel'yanenko, V. N.; Turovtsev, V. V.; Fedina, Y. A. Thermodynamic Properties of  
667 Pyruvic Acid and Its Methyl Ester. *Thermochim. Acta* **2018**, *665*, 70–75. doi:  
668 10.1016/j.tca.2018.05.009.
- 669 (97) Soonsin, V.; Zardini, A. A.; Marcolli, C.; Zuend, A.; Krieger, U. K. The Vapor Pressures  
670 and Activities of Dicarboxylic Acids Reconsidered: The Impact of the Physical State of the  
671 Aerosol. *Atmos. Chem. Phys.* **2010**, *10* (23), 11753–11767. doi: 10.5194/acp-10-11753-  
672 2010.

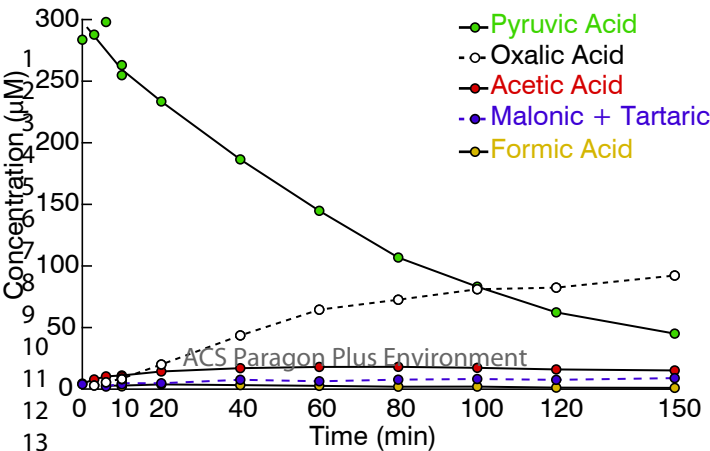
Manuscript for submission to *ACS Earth and Space Chemistry*

- 1  
2  
3 673 (98) Booth, A. M.; Barley, M. H.; Topping, D. O.; McFiggans, G.; Garforth, A.; Percival, C. J.  
4 674 Solid State and Sub-Cooled Liquid Vapour Pressures of Substituted Dicarboxylic Acids  
5 675 Using Knudsen Effusion Mass Spectrometry (KEMS) and Differential Scanning  
6 676 Calorimetry. *Atmos. Chem. Phys.* **2010**, *10* (10), 4879–4892. doi: 10.5194/acp-10-4879-  
7 677 2010.
- 8  
9  
10 678 (99) Paciga, A. L.; Riipinen, I.; Pandis, S. N. Effect of Ammonia on the Volatility of Organic  
11 679 Diacids. *Environ. Sci. Technol.* **2014**, *48* (23), 13769–13775. doi: 10.1021/es5037805.
- 12  
13  
14 680 (100) Pankow, J. F.; Asher, W. E. SIMPOL.1: A Simple Group Contribution Method for  
15 681 Predicting Vapor Pressures and Enthalpies of Vaporization of Multifunctional Organic  
16 682 Compounds. *Atmos. Chem. Phys.* **2008**, *8* (10), 2773–2796. doi: 10.5194/acp-8-2773-2008.
- 17  
18 683 (101) Gordon, B. P.; Moore, F. G.; Scatena, L.; Richmond, G. L. On the Rise: Experimental and  
19 684 Computational VSFS Studies of Pyruvic Acid and Its Surface Active Oligomer Species at  
20 685 the Air-Water Interface. *J. Phys. Chem. A* **2019**. doi: 10.1021/acs.jpca.9b08854.
- 21  
22  
23 686 (102) Bilde, M.; Barsanti, K.; Booth, M.; Cappa, C. D.; Donahue, N. M.; Emanuelsson, E. U.;  
24 687 McFiggans, G.; Krieger, U. K.; Marcolli, C.; Topping, D.; et al. Saturation Vapor Pressures  
25 688 and Transition Enthalpies of Low-Volatility Organic Molecules of Atmospheric Relevance:  
26 689 From Dicarboxylic Acids to Complex Mixtures. *Chem. Rev.* **2015**, *115* (10), 4115–4156.  
27 690 doi: 10.1021/cr5005502.
- 28  
29  
30  
31  
32  
33  
34  
35  
36  
37  
38  
39  
40  
41  
42  
43  
44  
45  
46  
47  
48  
49  
50  
51  
52  
53  
54  
55  
56  
57  
58  
59  
60

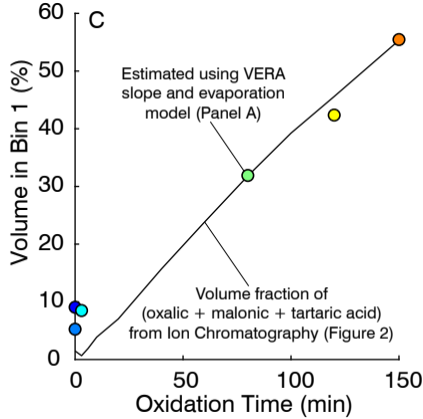
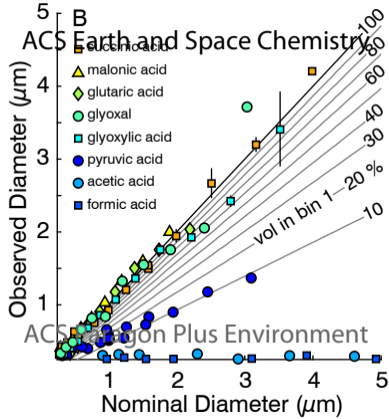
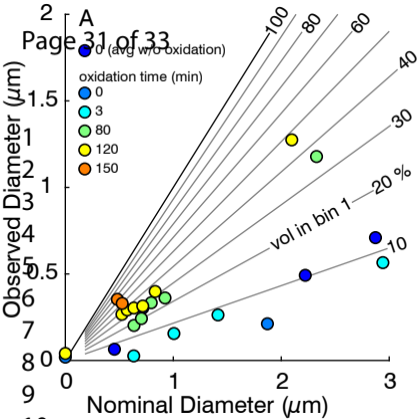
# Pyruvic Acid *in* Evaporating Droplets

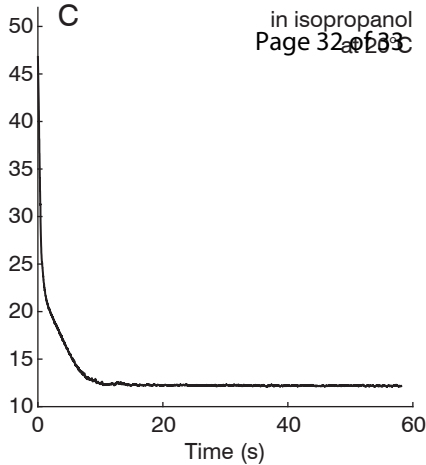
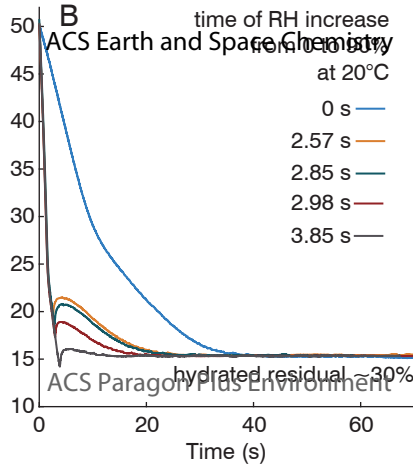
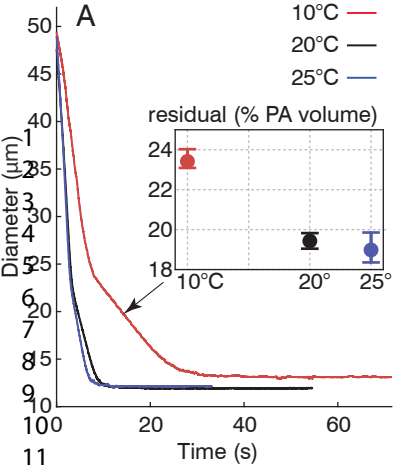
Page 29 of 33 ACS Earth and Space Chemistry











Volatile Organic Compounds (VOC)

Intermediate Volatility Organic Compounds (IVOC)

Semi-Volatile Organic Compounds (SVOC)

Low Volatility Organic Compounds (LVOC)

Extremely Low Volatility Organic Compounds (ELVOC)

